



ARL-TN-0824 MAY 2017

ARL

US Army Research Laboratory

Attempted α - to β -Phase Conversion of Croconic Acid via Ball Milling

by Steven W Dean, Rose A Pesce-Rodriguez, and Jennifer A Ciezak-Jenkins

Approved for public release; distribution is unlimited.

NOTICES

Disclaimers

The findings in this report are not to be construed as an official Department of the Army position unless so designated by other authorized documents.

Citation of manufacturer's or trade names does not constitute an official endorsement or approval of the use thereof.

Destroy this report when it is no longer needed. Do not return it to the originator.



Attempted α - to β -Phase Conversion of Croconic Acid via Ball Milling

**by Steven W Dean, Rose A Pesce-Rodriguez, and
Jennifer A Ciezak-Jenkins**
Weapons and Materials Research Directorate, ARL

REPORT DOCUMENTATION PAGE

Form Approved
OMB No. 0704-0188

Public reporting burden for this collection of information is estimated to average 1 hour per response, including the time for reviewing instructions, searching existing data sources, gathering and maintaining the data needed, and completing and reviewing the collection information. Send comments regarding this burden estimate or any other aspect of this collection of information, including suggestions for reducing the burden, to Department of Defense, Washington Headquarters Services, Directorate for Information Operations and Reports (0704-0188), 1215 Jefferson Davis Highway, Suite 1204, Arlington, VA 22202-4302. Respondents should be aware that notwithstanding any other provision of law, no person shall be subject to any penalty for failing to comply with a collection of information if it does not display a currently valid OMB control number.

PLEASE DO NOT RETURN YOUR FORM TO THE ABOVE ADDRESS.

1. REPORT DATE (DD-MM-YYYY) May 2017		2. REPORT TYPE Technical Note		3. DATES COVERED (From – To) August 2016 – May 2017	
4. TITLE AND SUBTITLE Attempted α - to β -Phase Conversion of Croconic Acid via Ball Milling				5a. CONTRACT NUMBER	
				5b. GRANT NUMBER	
				5c. PROGRAM ELEMENT NUMBER	
6. AUTHOR(S) Steven W Dean, Rose A Pesce-Rodriguez, and Jennifer A Ciezak-Jenkins				5d. PROJECT NUMBER	
				5e. TASK NUMBER	
				5f. WORK UNIT NUMBER	
7. PERFORMING ORGANIZATION NAME(S) AND ADDRESS(ES) US Army Research Laboratory ATTN: RDRL-WML-B Aberdeen Proving Ground MD 21005-5069				8. PERFORMING ORGANIZATION REPORT NUMBER ARL-TN-0824	
9. SPONSORING/MONITORING AGENCY NAME(S) AND ADDRESS(ES)				10. SPONSOR/MONITOR'S ACRONYM(S)	
				11. SPONSOR/MONITOR'S REPORT NUMBER(S)	
12. DISTRIBUTION/AVAILABILITY STATEMENT Approved for public release; distribution is unlimited.					
13. SUPPLEMENTARY NOTES					
14. ABSTRACT High-energy ball milling was used in an attempt to induce a high-pressure phase change in croconic acid (CA), which is being investigated as a potential novel energetic material. High-speed video of the milling process was analyzed to determine the peak pressures and impact durations experienced by the CA powder during milling. Differential scanning calorimetry was used to determine what effect varying the ball-to-sample mass ratio and milling time had on the energy content of the milled material. Results indicate the pressure achievable with currently available milling equipment is not sufficient to induce the desired α - to β -phase change, and extended milling times may degrade the material.					
15. SUBJECT TERMS ball milling, croconic acid, Hertzian stress, C ₅ H ₂ O ₅ , extended solid					
16. SECURITY CLASSIFICATION OF:			17. LIMITATION OF ABSTRACT UU	18. NUMBER OF PAGES 16	19a. NAME OF RESPONSIBLE PERSON Steven W Dean
a. REPORT Unclassified	b. ABSTRACT Unclassified	c. THIS PAGE Unclassified			19b. TELEPHONE NUMBER (Include area code) 410-278-6357

Contents

List of Figures	iv
List of Tables	iv
1. Introduction	1
2. Experimental	2
2.1 Ball Milling	2
2.2 High-Speed Video	2
2.3 Differential Scanning Calorimetry	3
3. Results and Discussion	3
3.1 Milling Pressures	3
3.2 Differential Scanning Calorimetry	7
4. Conclusions	8
5. References	9
Distribution List	10

List of Figures

Fig. 1	Molecular structure of CA	1
Fig. 2	ImageJ motion analysis of Wig-L-Bug during operation. White crosses represent the position of the center of the Wig-L-Bug clamp, and yellow markings denote the video frame at which the position was determined.....	4
Fig. 3	Plotted coordinates of Wig-L-Bug motion from Fig. 2. The y-movement is significantly greater in amplitude than the x-movement. The z-movement is not recorded in this video, but it is on the order of the x-movement.	5
Fig. 4	The y-component of Wig-L-Bug motion in time. The frequency is approximately 50 Hz, and the amplitude is approximately 2 cm.	6
Fig. 5	Peak pressure (p_{max}) and duration of impact (2τ) as a function of relative impact velocity for a stainless steel ball and vessel.	6
Fig. 6	Representative heat flow traces for milled CA samples. Curves have been offset to enhance clarity. Discontinuities in the traces are attributed to slight movement of the sample pans due to gas production by the sample and do not significantly affect energy release calculations.	7
Fig. 7	Energy released by the decomposition of CA, determined by integrating the DSC trace. Error bars represent 95% confidence intervals.....	8

List of Tables

Table 1	Parameters for milling experiments	2
Table 2	Values for Eqs. 1 and 2	4

1. Introduction

Croconic acid (CA, $C_2H_2O_5$, 4,5-dihydroxycyclopentenetrione) is a member of the family of oxycarbon acids, which includes deltic acid ($C_3H_2O_2$), squaric acid ($C_4H_2O_4$), and rhodizonic acid ($C_6H_2O_6$). The molecular structure of CA is shown in Fig. 1. Recent research conducted at the US Army Research Laboratory identified a high-pressure polymorph of CA (β -CA), which has been suggested to have high-energy density and may have applications as a propellant.¹

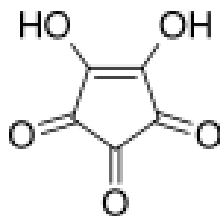


Fig. 1 Molecular structure of CA (This image is copied from Wikipedia in the public domain and is free of copyright and can be used without any license requirements. https://en.wikipedia.org/wiki/Croconic_acid.)

Large-scale production of β -CA is hindered by the high pressures necessary to induce the α - to β -phase change. In a Paris Edinburg large-volume press, the β -CA polymorph was synthesized through the compression of as-received, α -CA to 9 GPa for a minimum of 24 h; slightly lower transition pressures have been noted in the diamond anvil cell.² The necessity of the high pressure in its synthesis limits the annual production of β -CA, using one Paris Edinburg cell, to approximately 13 g/yr.¹ Previous research investigated a potential means of increasing production via water-recrystallization.¹ Such methods were found to be unsuccessful, with the initial color shift of CA, which was previously determined to be indicative of the α - to β -phase change, found to be a particle-size effect and not a result of the desired phase change.

This report investigates efforts to synthesize β -CA through ball milling. In ball milling, high pressures are generated by the impact of a ball with a vessel wall while the vessel is agitated. This method is well established in the literature as a technique to induce mechanical alloying in the production of nano-crystalline materials³ and reactive materials.⁴ It was hoped that the dynamic pressures generated during milling would allow for rapid production of β -CA, but this was found to not be the case.

2. Experimental

2.1 Ball Milling

Several kinds of ball mills are commonly used in material processing including attritor mills, rolling ball mills, and planetary ball mills. This study used a vibratory ball mill; such mills consist of a vessel containing a ball that is moved rapidly back and forth, resulting in the ball colliding with the ends of the vessel on each swing.

A Wig-L-Bug (Dentsply Rinn) ball mill was used to induce high dynamic pressures in as-received CA powder. The Wig-L-Bug is similar in many respects to the commonly used “SPEX-type” high-energy ball mill but on a smaller scale. The vessel and ball in the Wig-L-bug are both stainless steel. The ball has a diameter of 6.35 mm and a mass of 1 g; the vessel outer diameter is 12.7 mm, and the vessel length is 27.7 mm. A series of milling experiments were conducted, varying the ball to sample mass ratio and the amount of milling time. Experiments conducted are summarized in Table 1.

Table 1 Parameters for milling experiments

Sample no.	Ball-to-sample mass ratio	Mill time (min)
0 (control)	NA	0
1	20:1	1
2	10:1	1
3	5:1	1
4	10:1	5
5	10:1	10

NA = not applicable

2.2 High-Speed Video

A Fastcam SA-Z (Photron) high-speed digital video camera was used to record the motion of the Wig-L-Bug ball mill; from this motion it was possible to determine the velocity parameters needed for Hertzian stress calculations. A small piece of tape was placed on the mill to aid in motion tracking. The mill was activated and then the camera was triggered to record its motion. The frame rate of the camera was 5000 fps and the exposure time was 199 μ s.

2.3 Differential Scanning Calorimetry

Differential scanning calorimetry (DSC) experiments were conducted to determine how milling effected the CA powder. A Q2000 DSC (TA Instruments) was used to heat a small sample of material at 10 °C /min from ambient temperature to 475 °C. During the heating process, the furnace was purged with nitrogen flowing at 100 mL/min. Three DSC traces were collected for each sample.

3. Results and Discussion

3.1 Milling Pressures

The high pressures achievable in this type of mill result from stresses that develop in the milled material as it is trapped between the ball and end wall. These contact stresses were first studied by Hertz⁵ and referred to as Hertzian stresses.⁶ Maurice and Courtney⁷ applied the concept of Hertzian stresses to high-energy ball milling to determine the parameters important to mechanical alloying. They determined an expression for the maximum pressure achieved in a mill, given in Eq. 1 as

$$p_{max} = g_p v^{0.4} (\rho/E_{eff})^{0.2} E_{eff} \quad (1)$$

and an expression for the total duration of the ball-wall impact event (2τ), given in Eq. 2 as

$$2\tau = g_\tau v^{-0.2} (\rho/E_{eff})^{0.4} R, \quad (2)$$

where p_{max} is the maximum pressure, g_p and g_τ are geometric constants, v is the relative ball-wall velocity, ρ is the ball density, E_{eff} is the effective tensile modulus of the ball and container, and R is the ball radius. In this study, the ball and container are both made of the same material, so the effective modulus is the tensile modulus of stainless steel. The values of these parameters are listed in Table 2. The values of g_p and g_τ are for a ball impacting a flat surface, which was deemed to be an acceptable approximation given the large difference in radius of curvature between the ball and vessel ends.

Table 2 Values for Eqs. 1 and 2^{7,8}

Parameter	Value	Unit
g_p	0.3521	...
g_τ	6.4034	...
ρ	7450	kg/m ³
E_{eff}	210×10^9	Pa
R	3.18×10^{-3}	m

To determine the impact velocity of the ball on the end wall of the Wig-L-Bug, a high-speed video of the mill in motion was imported into ImageJ (National Institutes of Health) for image analysis. The video was advanced frame-by-frame and the leading edge of the small piece of tape placed on the mill clamp was determined in each frame. A screen capture from ImageJ after motion analysis is shown in Fig. 2.

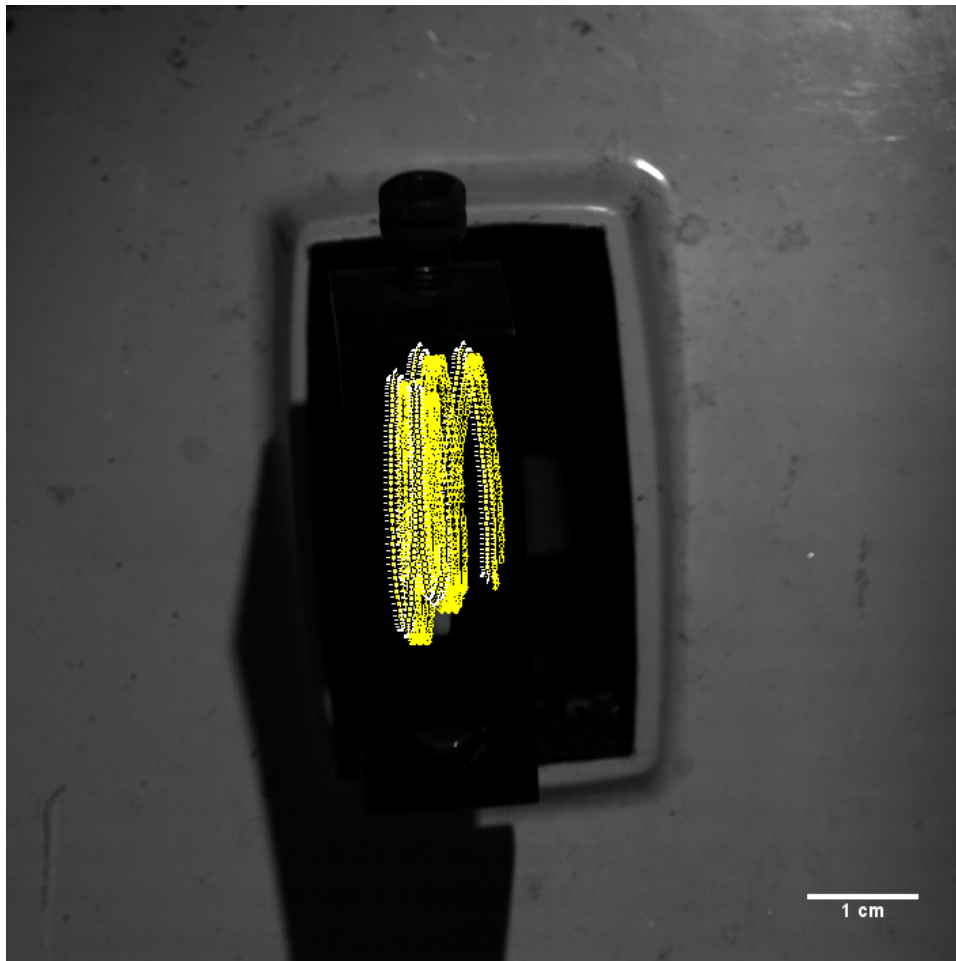


Fig. 2 ImageJ motion analysis of Wig-L-Bug during operation. White crosses represent the position of the center of the Wig-L-Bug clamp, and yellow markings denote the video frame at which the position was determined.

The coordinates determined by motion analysis are plotted in Fig. 3. The motion of the mill is 3-dimensional (with the z-component not recorded), but the x- and z-components of the motion are significantly smaller than the y-component. To simplify analysis, only the y-component of the motion was used to determine the relative impact velocity.

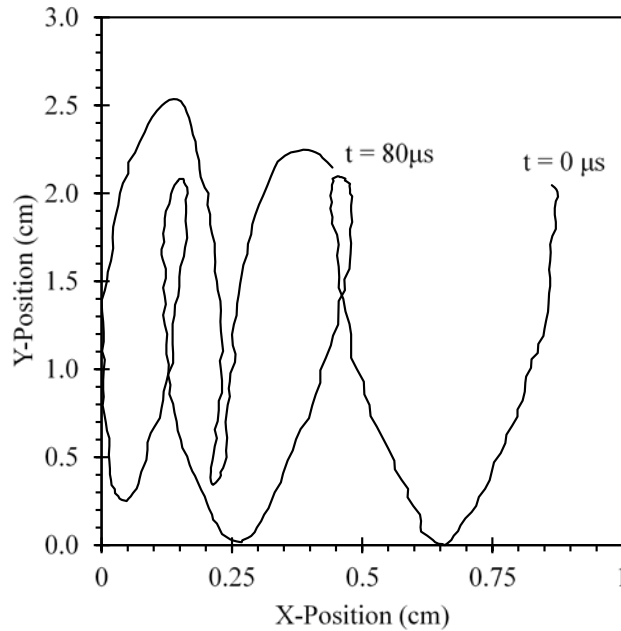


Fig. 3 Plotted coordinates of Wig-L-Bug motion from Fig. 2. The y-movement is significantly greater in amplitude than the x-movement. The z-movement is not recorded in this video, but it is on the order of the x-movement.

The relative impact velocity was calculated using the relationship developed by Maurice and Courtney for a SPEX-type mill, given in Eq. 3 as⁷

$$v = 2x/t \quad (3)$$

where v is the relative impact velocity, x is the distance traveled by the mill in one full vibration cycle (i.e., twice the amplitude), and t is the time of one milling cycle.

Plotting the y-component of the motion of the mill (Fig. 4), the frequency of the mill is approximately 50 Hz, and the amplitude of the motion is approximately 2 cm. Thus $x = 0.04$ m and $t = 0.02$ s, roughly. When Eq. 3 is used, this results in a relative impact velocity of $v \approx 4$ m/s. At this impact velocity the peak impact pressure is 4.2 GPa, and the impact duration is 1.6 μ s.

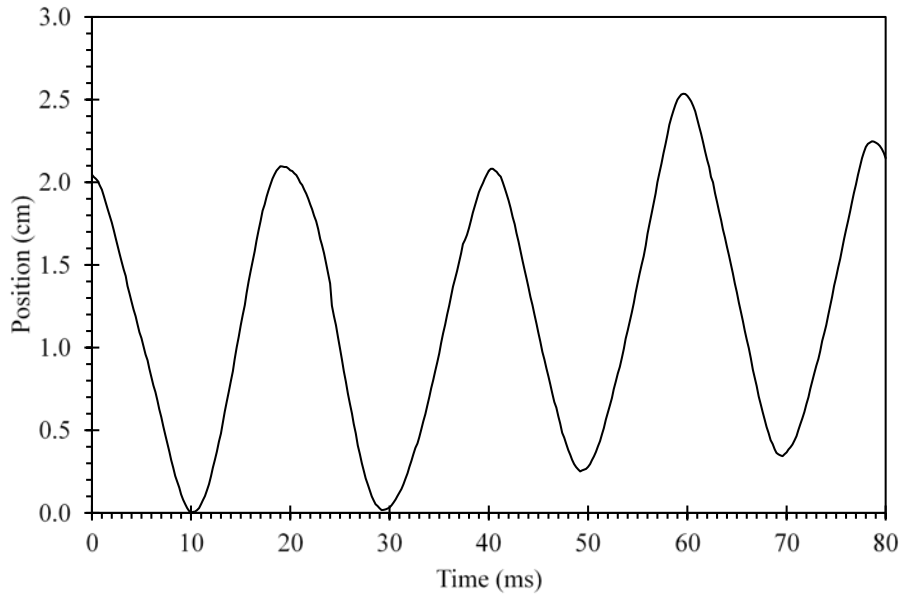


Fig. 4 The y-component of Wig-L-Bug motion in time. The frequency is approximately 50 Hz, and the amplitude is approximately 2 cm.

The maximum pressure and duration of impact over a range of impact velocities, calculated using Eqs. 1 and 2 with the parameters listed in Table 2, are plotted in Fig. 5. The velocity needed to reach 9-GPa peak pressure is approximately 28 m/s, which has an impact duration of 1.1 μs .

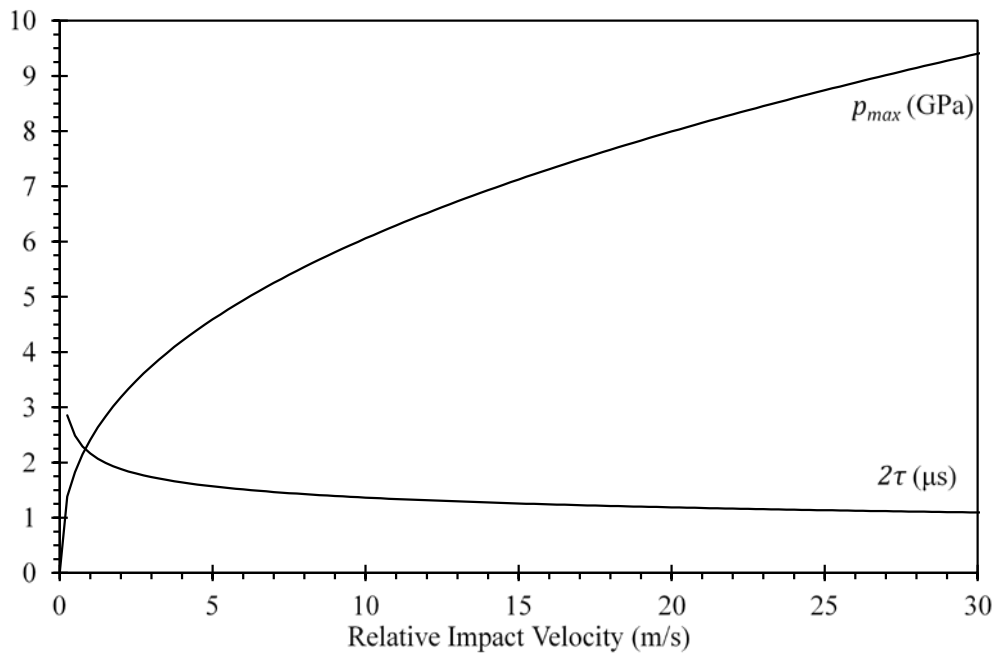


Fig. 5 Peak pressure (p_{max}) and duration of impact (2τ) as a function of relative impact velocity for a stainless steel ball and vessel

3.2 Differential Scanning Calorimetry

Representative heat flow traces showing the exothermic decomposition of CA samples are shown in Fig. 6. The integrated exotherm areas for all samples are shown in Fig. 7. From these figures, it is apparent that varying the ball to sample mass ratio (Samples 1–3) did not have an effect on the resulting exothermicity of the milled material compared to the control sample (Sample 0), and extending the milling time had only a moderate effect. Samples milled for 5 min (Sample 4) showed somewhat higher exothermicity than the control sample but with significant variation in the results. Samples milled for 10 min (Sample 5) showed a significant reduction in exothermicity, again with large variation. This may be due to sample degradation caused by elevated temperatures induced by frictional heating in the mill.

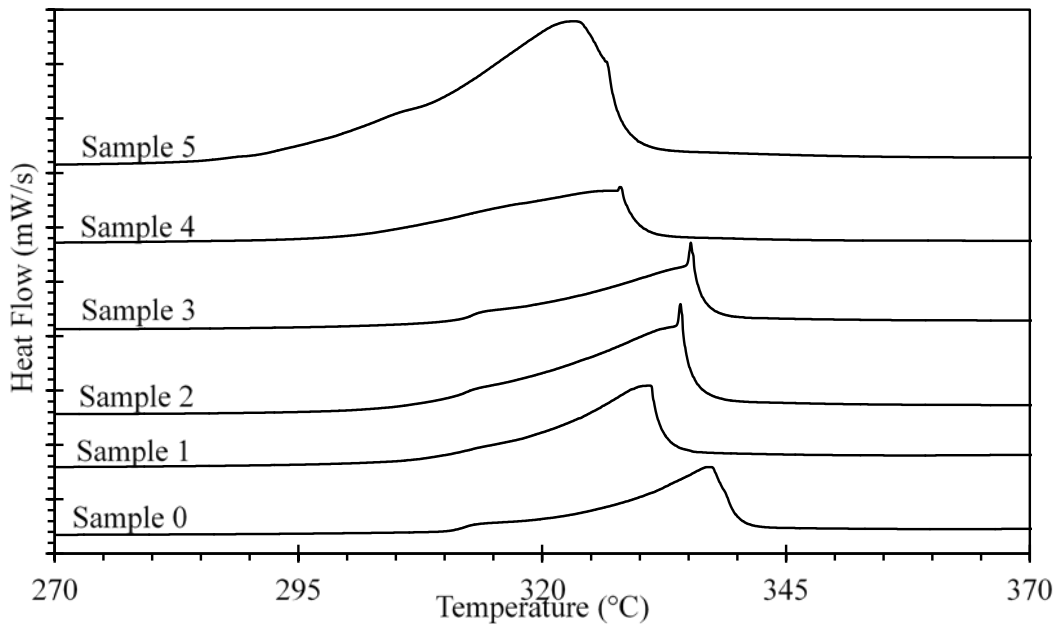


Fig. 6 Representative heat flow traces for milled CA samples. Curves have been offset to enhance clarity. Discontinuities in the traces are attributed to slight movement of the sample pans due to gas production by the sample and do not significantly affect energy release calculations.

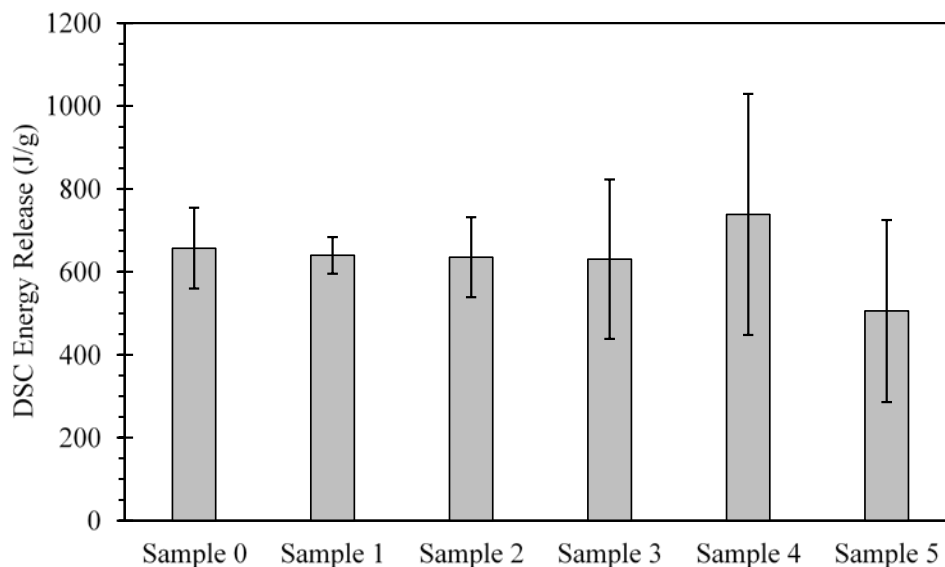


Fig. 7 Energy released by the decomposition of CA, determined by integrating the DSC trace. Error bars represent 95% confidence intervals.

4. Conclusions

From the DSC measurements, it is apparent that the currently available milling equipment is likely not an effective method to induce the desired phase change α - to β -CA. This agrees with the pressures and impact durations calculated based on high-speed video analysis of the Wig-L-Bug. The pressures achievable with this small mill are less than half that required to induce the phase change. These pressures are also only sustained for times on the order of microseconds, rather than the several hours long duration currently employed.

Higher pressures could be achieved by increasing the relative impact velocity of the mill or by modifying the mill/ball materials. However, due to the very short impact durations of ball milling it is likely that pressures significantly greater than 9 GPa would be required. It will also be important to minimize heat generation caused by milling to prevent material decomposition. This may be possible through the use of cryogenic milling.

5. References

1. Isert S, Ciezak-Jenkins J. Investigation and characterization of water-recrystallized croconic acid. Aberdeen Proving Ground (MD): Army Research Laboratory (US); 2016 Dec. Report No.: ARL-TR-7910.
2. Ciezak-Jenkins J, Jenkins T. The high-pressure characterization of carbon oxides: croconic acid. Aberdeen Proving Ground (MD): Army Research Laboratory (US); 2014 June. Report No.: ARL-TR-6957.
3. Suryanarayana C. Mechanical alloying and milling. *Progress in Mat Sci.* 2001;46(1):1–184.
4. Schoenitz M, Ward TS, Dreizin EL. Fully dense nano-composite energetic powders prepared by arrested reactive milling. *Proceedings of the Combustion Institute.* 2005;30(2):2071–2078.
5. Hertz H. *Miscellaneous papers.* 1896: Macmillan.
6. Shigley JE, Mischke CR, Budynas RG. *Mechanical engineering design.* New York (NY): McGraw-Hill; 2004.
7. Maurice DR, Courtney T. The physics of mechanical alloying: a first report. *Metallurgical Transactions A.* 1990;21(1):289–303.

1 DEFENSE TECHNICAL
(PDF) INFORMATION CTR
DTIC OCA

2 DIRECTOR
(PDF) US ARMY RESEARCH LAB
RDRL CIO L
IMAL HRA MAIL & RECORDS
MGMT

1 GOVT PRINTG OFC
(PDF) A MALHOTRA

3 DIR USARL
(PDF) RDRL WML B
S DEAN
R PESCE-RODRIGUEZ
J CIEZAK-JENKINS